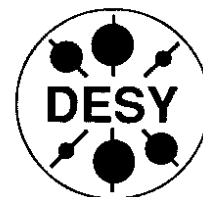


**DEUTSCHES ELEKTRONEN-SYNCHROTRON**



DESY 95-140  
July 1995



**Selected Topics of Deep Inelastic Scattering  
from the Sixties to HERA**

J. Gayler

*Deutsches Elektronen-Synchrotron DESY, Hamburg*

ISSN 0418-9833

**NOTKESTRASSE 85 - 22607 HAMBURG**

DESY behält sich alle Rechte für den Fall der Schutzrechtserteilung und für die wirtschaftliche Verwertung der in diesem Bericht enthaltenen Informationen vor.

DESY reserves all rights for commercial use of information included in this report, especially in case of filing application for or grant of patents.

To be sure that your preprints are promptly included in the  
HIGH ENERGY PHYSICS INDEX,  
send them to (if possible by air mail):

**DESY**  
Bibliothek  
Notkestraße 85  
22607 Hamburg  
Germany

**DESY-IfH**  
Bibliothek  
Platanenallee 6  
15738 Zeuthen  
Germany

$$\frac{d^2\sigma}{dx dy} = \frac{G_F^2}{2\pi} \frac{M_W^4}{(Q^2 + M_W^2)^2} s \times$$

$$[(1-y)F_2(x, Q^2) + y^2 x F_1(x, Q^2) \pm (y-y^2/2)xF_3(x, Q^2)]$$

In neutral current (NC) interactions of charged leptons the parity violating structure function  $F_3$  can be neglected in most experiments due to dominance of virtual photon exchange. In this case the corresponding formula is obtained by replacing  $\frac{G_F^2}{2\pi} \frac{M_W^4}{(Q^2 + M_W^2)^2}$  by  $4\pi\alpha^2/Q^4$ .

The structure functions  $F_2$  and  $F_1$  are related by  $(F_2 - 2xF_1)/2xF_1 = R$ , where  $R = \sigma_l/\sigma_t$  is the ratio of cross sections of longitudinally and transversely polarized virtual photons.

In the present talk I do not attempt to give a systematic review. I rather select some topics which I find especially important and interesting or which are directly related to present work at HERA.

The paper is structured as follows:

In section 2 the experiments are shortly discussed which led to the discovery of Bjorken scaling and the point like constituents in the nucleon, followed by the first evidence for scaling violations. Section 3 reports on some very early statements concerning gluons. The discovery of nuclear effects in lepton scattering is recalled in section 4. Recent fixed target results, especially on the Gottfried and Gross-Llewellyn Smith sum rules, followed by results on structure functions obtained at HERA are discussed in sections 5 and 6. Section 7 reports on early jet observations up to the determination of  $\alpha_s$  from jet rates at HERA. Finally I present in section 8 results on electroweak effects in electron scattering from SLAC in 1978 and from HERA.

## 2. From First Indications of Scaling to Scaling Violations

### 2.1. The Time before Observation of Scaling

In the sixties electron scattering experiments were performed at various labs detecting the electrons in magnetic spectrometers of small acceptance (typically 1 msr and about 10% in momentum). The first interest was, in the tradition of Hofstadter's form factor measurements, to explore elastic  $ep$  scattering. Before SLAC came to operation, it was shown that the nucleon form factors decreased rapidly with  $Q^2$ , in particular the magnetic form factor of the proton,  $G_M(Q^2)$ , was well described by the "dipole formula"

$$G_M(Q^2) = 1/(1 + Q^2/0.71 GeV^2)^2$$

up to  $Q^2 \approx 10 GeV^2$  [2]. But no deep insight resulted from these analyses at the time, especially no hint for point like nucleon substructures.

Lowering the magnet current of the spectrometers, higher mass final states could be observed showing resonance structures familiar from pion-nucleon scattering. Typical energy spectra taken at CEA in 1967 [3] at different incident energies but fixed scattering angle are shown in figure 1.

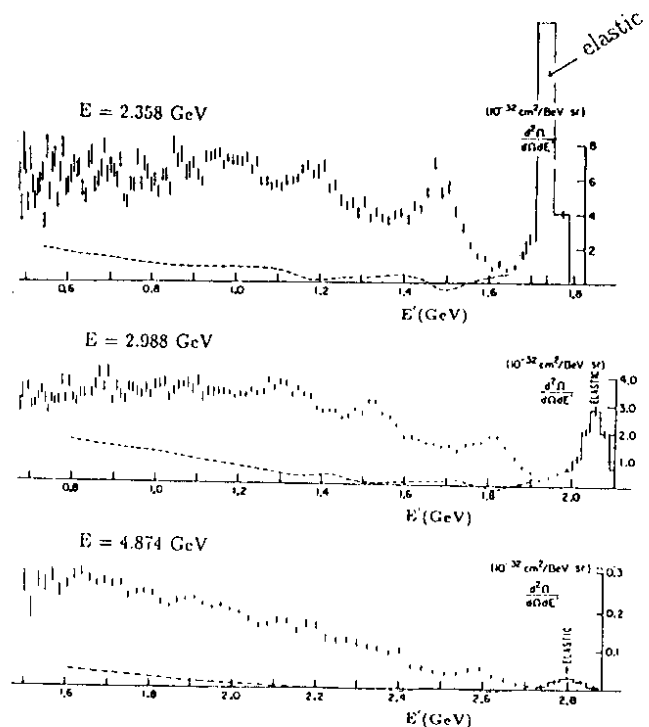


Figure 1. Energy spectra of scattered electrons at  $\theta = 31^\circ$ , with different primary energies, (CEA, 1967 [3])

At that time there was no general understanding how nuclear constituents like quarks might manifest themselves in such data (although the basic concept of scaling was anticipated by Bjorken already in 1966 [4], see C. Llewellyn Smith, these proceedings). It is however interesting to note, that already these data showed patterns which were later interpreted as the effect of point like substructures of the nucleon. The elastic peak vanishes much more rapidly with increasing  $Q^2$  than the higher resonances or the inelastic continuum at  $W \gtrsim 2 GeV$ . It was explicitly pointed out by a DESY-group [5], that the higher the value of  $W$ , the slower the decrease with  $Q^2$ , quite different from the naive expectation from elastic form factors.

### 2.2. Observation of Scaling

The break-through came with the data from SLAC presented by W. Panofsky at Vienna, 1968 [6]. They were taken at higher energies than available before and showed (figure 2) that the structure function  $F_2$  approximately was a function of  $x$  only, independent of  $Q^2$  ("scaling"), as expected by Bjorken [4, 7].

The relevance of this observation was well seen and considered as "indicative that point-like interactions are being involved" [6].

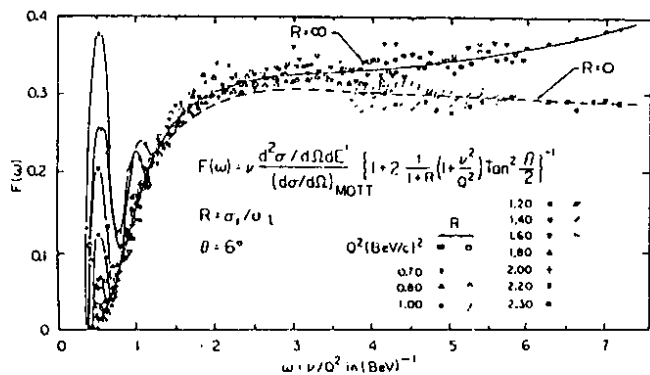


Figure 2. First observation of scaling,  $0.7 < Q^2 < 2.3 \text{ GeV}^2$ , assuming  $R = 0$  and  $R = \infty$ . SLAC data, 1968[6]

In 1969 more data were available from SLAC [8], showing scaling in a wider kinematic range. The concept of point-like constituents was nicely supported also by pictures like figure 3 [8], showing that indeed the inelastic cross sections behave as expected from point charges, contrary to the elastic ones. In the latter case the electron scatters off an extended object which is kept intact in the interaction, corresponding to a rapidly falling proton form factor.

These findings at SLAC changed the perspectives at DESY considerably and approximate scaling could now be observed also there, but with inferior quality due to lack of electron energy [9].

### 2.3. Spin of the Constituents

Very important conclusions on the spin of the proton constituents could be drawn already in 1969. The data showed that the ratio  $R = \sigma_l/\sigma_t$  is small which is expected for spin 1/2 quarks (Callan Gross rule [10]).

This conclusion was possible by combining large angle data from DESY with small angle data from SLAC (figure 4), and also by interpolation of SLAC data alone, as presented first at the Electron Photon Conf. at Liverpool by R. Taylor [11].

### 2.4. First Observation of Scaling Violations

The concept of spin 1/2 constituents of the hadrons was finally established by the results of  $ep$  scattering discussed above. Before, quarks were rather a tool to classify hadrons, now they were more directly felt in scattering processes. The remaining deviations from scaling led to efforts to find better scaling variables besides,  $\omega = 1/x$ , with the aim to extend the kinematic range where scaling holds [12].

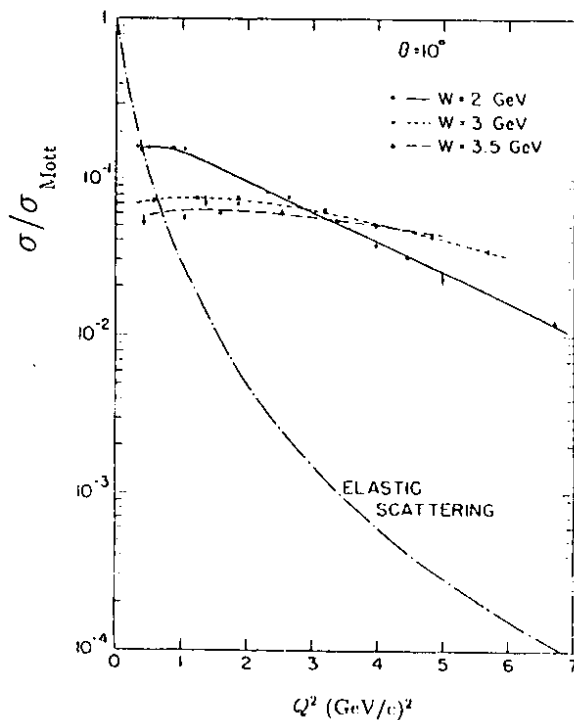


Figure 3.  $d^2\sigma/d\Omega dE'/\sigma_{\text{Mott}}$  vs.  $Q^2$ . Inelastic and elastic data from SLAC [8], 1969

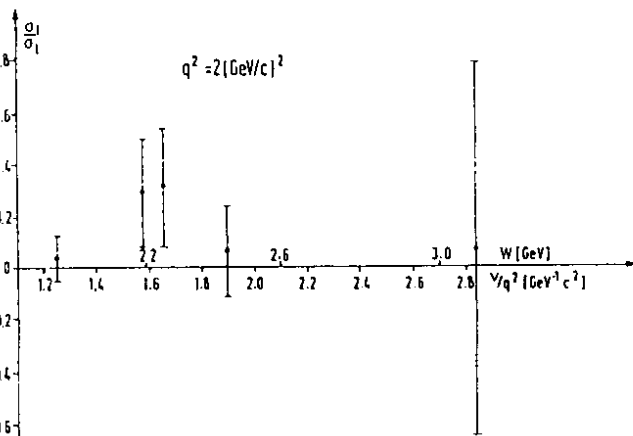


Figure 4.  $R = \sigma_l/\sigma_t$ , DESY/SLAC, 1969 [11].

The important experimental effort was however to test the scaling hypothesis seriously at high energies. This was possible in the new  $\mu$  beam line at Fermilab and led to first results in 1974 [13]. The experiment was carefully designed especially for such a test. Muons incident on an iron target were measured in a magnetic spectrometer. The data had been taken at two beam energies, 56.3 GeV and 150 GeV, with the apparatus changed such that the acceptance and resolution in  $x$  stayed the same for the two cases with  $Q^2$  scaling by the energy ratio (150/56.3). This was achieved by

changing appropriately the length of the spectrometer, by introducing dummy material to increase multiple scattering at the high energy run. Even the target length was changed such as to keep the event rate constant if scaling holds.

The results (figure 5) showed for the first time the by now familiar pattern: at high  $x$  the cross section decreases faster with  $Q^2$  than expected from scaling and the opposite at low  $x$ .

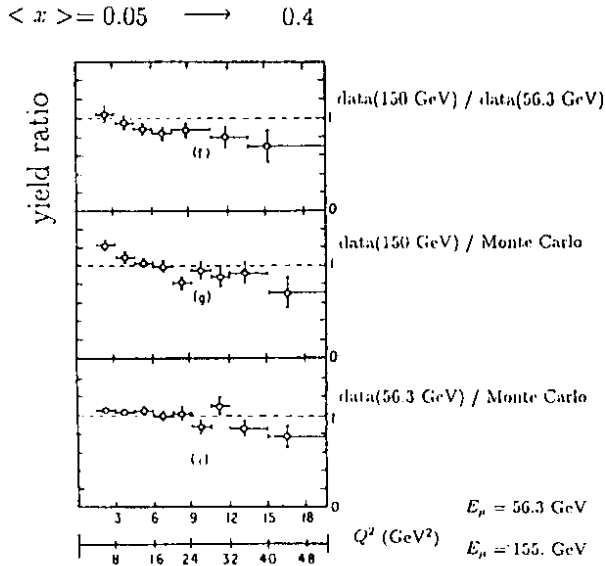


Figure 5. Scaling violations [13], 1974. Event ratio at same  $x$ , different  $Q^2$ . The data are also compared with a simulation assuming scaling.

Scaling violations were later confirmed by SLAC [14] and further results from Fermilab [15].

### 3. The Appearance of Gluons

Already before the development of QCD and before the observation of scaling violations gluons entered the game via the sum  $\int F_2 dx$ . Its experimental value led to the conclusion that there are not just charged quarks in the nucleon. It is interesting to note some early statements in that context:

- In 1969 Bjorken and Paschos [16] studied this integral and expected for the proton in a simple model, with  $N$  partons (valence plus symmetric sea) of charges  $q_i$ , having equal momentum distributions

$$\int_0^1 F_2 dx = \langle q_i^2 \rangle = [1 + \frac{2}{9}(N - 3)]/N \quad ,$$

i.e.  $1/3$  for just 3 valence quarks. In view of the experimental data they then stated: “numerically  $\int dx F_2 \approx 0.16$ , yielding a rather small mean-square

charge per parton”, but refrained from any further comment.

- In 1970 Llewellyn Smith [17], based on the same arithmetic, stated that the data allow for “neutral partons” with fraction  $c'$  of the non-valence “background” with  $c' > 0.28$  and  $1/\langle N \rangle < 0.16$ .
- In 1971 Kuti and Weisskopf [18] remarked, that there is “evidence for the presence of uncharged partons (gluons) within the proton (Feynman, private communication)” and derived that “about  $1/3$  of the momentum is carried by gluons”.

Meanwhile we know that about half of the nucleons momentum is carried by gluons. The Gargamelle bubble chamber reported 1975 [19] a value of  $\int_0^{0.8} F_2 dx = 0.47 \pm 0.02$  from  $\nu$  Freon data. Here the integral corresponds directly to the gluon momentum fraction. Similarly an early QCD analysis [20] using Fermilab and SLAC data gave a gluon momentum fraction of 0.44 at  $Q^2 = 10 \text{ GeV}^2$ .

Later, on the basis of  $\nu$  data [21] from BEBC and CDHS besides the Fermilab  $\mu$  data [15], the slow decrease of  $\int F_2 dx$  with  $Q^2$  was considered as a triumph of QCD, as it excluded theories with scalar gluons or non-abelian vector gluons [22].

### 4. Nuclear Effects

One of the big surprises in lepton scattering was the discovery reported in 1983 [23] by the European Muon Collaboration (EMC) that iron nuclei appear not simply as the sum of their nucleons with some effects of Fermi motion: the nuclear environment modifies the effective  $x$  distribution of the quarks, seen by the scattered muon, as shown in figure 6, in which  $F_2$  per nucleon is compared for iron and deuterium targets [23].

This observation was not the result of a dedicated experiment. EMC had started its program in 1979 with an iron target. Then nearly one year later, after a series of runs on hydrogen, EMC took data with a deuterium target, with the main aim to measure  $n/p$  cross section ratios. So it was not straight forward to decide on the basis of a small observed effect (about  $\pm 10$  to 15%) that an unexpected physics phenomenon was discovered, and it was only after long systematic studies and heavy internal discussions that EMC proceeded to publish in January 1983.

It was even more surprising that the result was confirmed only one month later by A. Bodek et al. [24]. They were able to reanalyse extremely fast old data taken about 10 years before by the experiment E87 at SLAC. In particular the control runs with empty steel and aluminium vessels of the deuterium targets allowed to study Fe/D [24] and Al/D ratios [25] (figure 7). Besides the agreement with EMC, the effect of Fermi

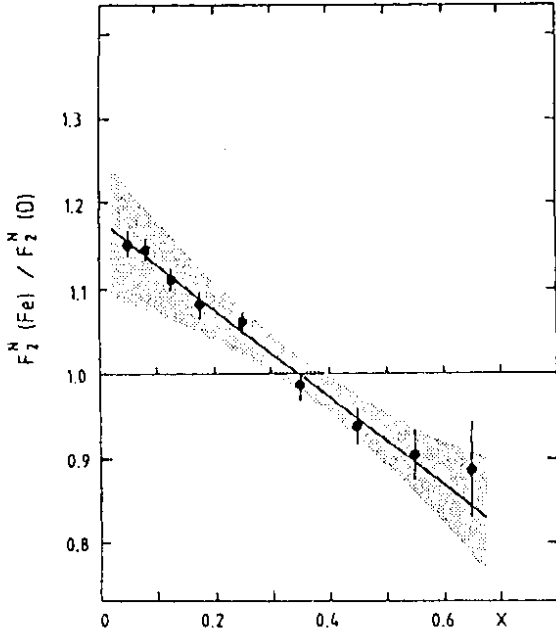


Figure 6. Ratio of  $F_2$  per nucleon for iron and deuterium as measured by EMC [23], 1983. The shaded area indicates the effect of systematic errors on the slope.

smearing could nicely be observed at large  $x$ .

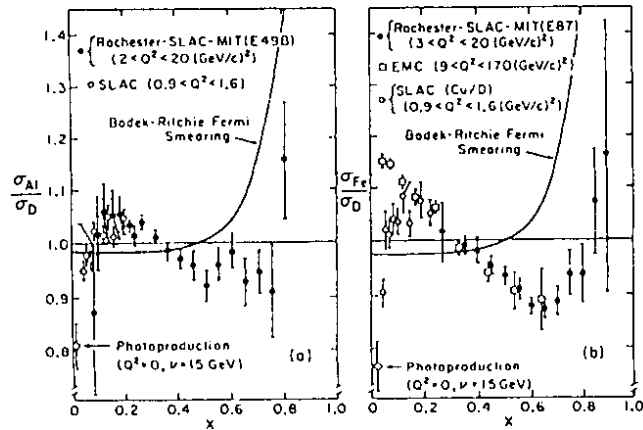


Figure 7. Confirmation of the "EMC effect" by ratios  $\sigma(A)/\sigma(D)$  and  $\sigma(Fe)/\sigma(D)$ , SLAC [24, 25], 1983.

The surprising result and its rapid confirmation led in the following years to an industry of both, experimental and theoretical work on the "EMC-effect". Dedicated experiments followed at SLAC and the collaborations BCDMS, EMC, NMC at CERN and E665 at Fermilab. Now precise data are available (see e.g. figure 8 [26]) for many nuclei, spanning a large range of  $x$  (down to  $\lesssim 10^{-4}$ ) and  $Q^2$ .

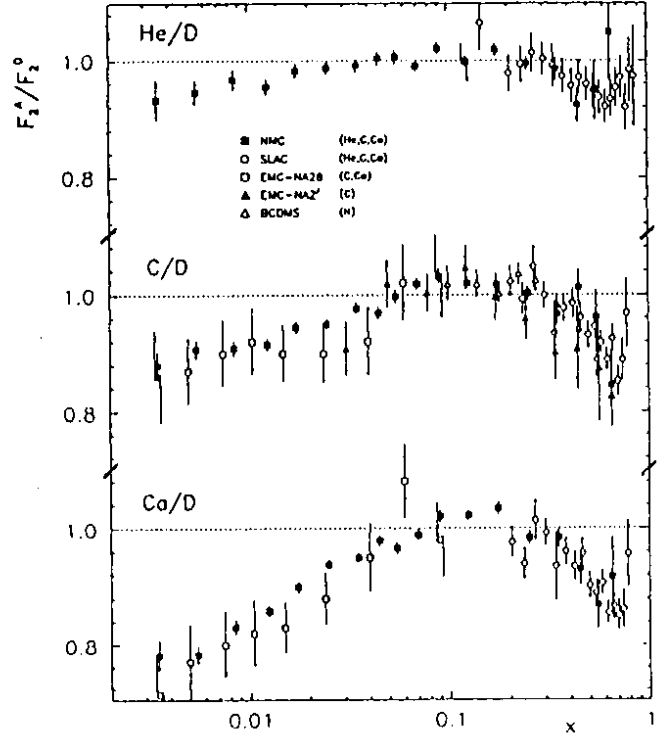


Figure 8.  $F_2^A/F_2^D$  vs.  $x$  with  $A = He, C$  and  $Ca$ . Results from NMC, SLAC and BCDMS, from [26], 1991.

Some main characteristics:

- There is little or no  $Q^2$  dependence of  $\sigma(A)/\sigma(D)$ .
- Nuclear shadowing is observed for  $x \lesssim 0.04$ .
- The ratio  $\sigma(A)/\sigma(D)$  increases with  $A$  between  $x \approx 0.1$  and  $x \approx 0.2$  and then decreases with  $A$  at larger  $x$ . The effects of Fermi motion get visible at  $x \gtrsim 0.7$ .
- There is little or no dependence of  $R = \sigma_l/\sigma_t$  on  $A$ .

The very first theoretical papers, appearing soon after the EMC publication, aimed for an explanation of the effect in terms of enhanced pion clouds in nuclei, which lead to more  $q\bar{q}$  pairs for  $x < M_\pi/M_p$  [27].

It goes far beyond the scope of this talk to cover the present theoretical and experimental situation. I refer to the excellent review of M. Arneodo [28] and the discussions of this workshop [29].

## 5. Recent Fixed Target Data

There is a wealth of data available from inclusive  $e$ ,  $\mu$  and  $\nu$  scattering, from "fixed targets", which beautifully confirm with very high precision the patterns of scaling violation as predicted by QCD. The most precise data, which are now mainly used in QCD analyses, are from SLAC ( $eN$ ) and the BCDMS, NMC ( $\mu N$ ) and CCFR ( $\nu N$ ) collaborations. Other experiments have either little statistical weight or larger systematic

uncertainties. There exist comprehensive recent reviews by M. Virchaux [30], R. Voss [31] and J. Feltesse [32]. New  $\mu N$  data, especially at low  $x$ , are coming from the E665 collaboration [33].

In somewhat more detail I will only discuss recent results on the Gross-Llewellyn Smith sum rule and on the Gottfried sum rule.

### 5.1. Gottfried Sum and Flavour Symmetry

The Gottfried sum [34]

$$S_G \equiv \int_0^1 (F_2^p - F_2^n) \frac{dx}{x}$$

can be expressed in the quark parton model, assuming isospin invariance, in terms of quark densities as

$$S_G = 1/3 + 2/3 \int_0^1 (\bar{u}(x) - \bar{d}(x)) dx$$

which reduces to the valence quark contribution 1/3 for a flavour symmetric sea. The results (figure 9) obtained 1991 by NMC and an improved analysis in 1994 [35] show that the QPM value of 1/3 is by far not reached in the covered  $x$  range leading to

$$\int_0^1 (\bar{u}(x) - \bar{d}(x)) dx = -0.147 \pm 0.039$$

which implies, that there is more sea of  $d$  than of  $u$  flavour in the proton.

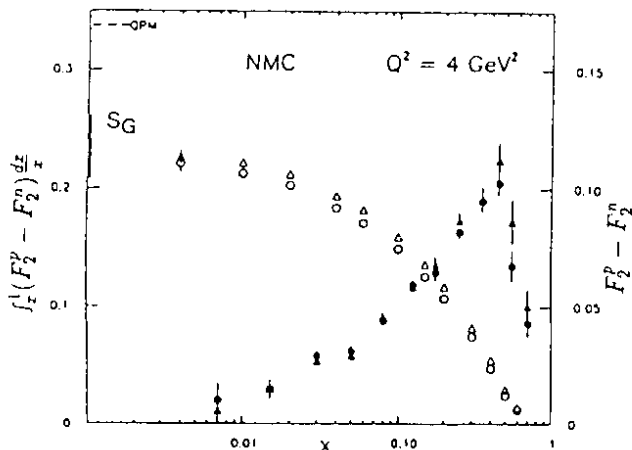


Figure 9.  $F_2^p - F_2^n$  (full symbols) and  $\int_{x_{min}}^1 (F_2^p - F_2^n) dx/x$  (open). NMC, 1991 (triangles) and 1994 (circles) [35].

That the  $d$ -sea exceeds that of  $u$  was recently also concluded from the measured asymmetry of Drell Yan production on  $p$  and  $n$  targets [36] and the  $W^\pm$  charge asymmetry in  $p\bar{p}$  collisions [37]. The results had considerable impact on parton density parametrizations.

Acceleration of deuterium nuclei at HERA [38] would allow to extend the test of the Gottfried sum rule to much smaller  $x$  and would therefore reduce very much the remaining uncertainty in the extrapolation to  $x = 0$  in the NMC results.

### 5.2. Gross-Llewellyn Smith Sum Rule

This sum rule, derived in 1969 [39], states that

$$S_{GLS} \equiv \int_0^1 F_3(x) dx = 3$$

As the quark content of  $F_3$  is the sum over  $q_i(x) - \bar{q}_i(x)$ , the sum measures the number of valence quarks.

The sum rule is interesting at present for two reasons:

- There exist very precise data from CCFR [40]:  $S_{GLS} = 2.50 \pm 0.018 \pm 0.078$  at  $Q^2 = 3 \text{ GeV}^2$ , obtained from the difference of  $\nu$  and  $\bar{\nu}$  cross sections on iron (figure 10).
- There exist next to next to leading order QCD corrections [41, 42] to the sum rule which allow for a precise determination of  $\alpha_s$ , the strong coupling constant, at small  $Q^2$ .

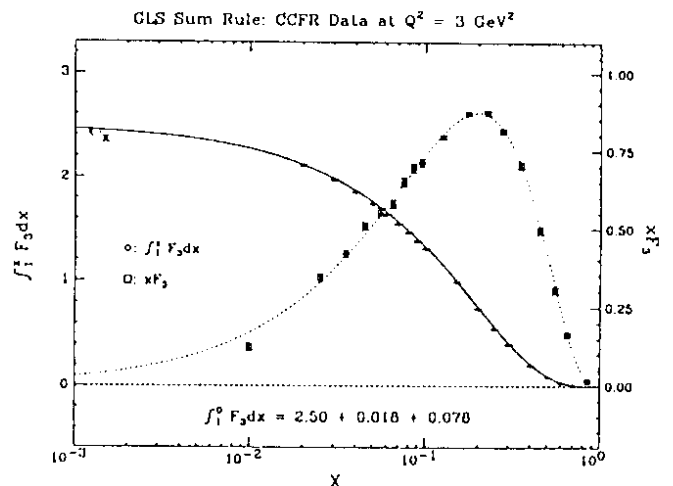


Figure 10.  $F_3$  (open symbols) and  $\int_1^x F_3 dx$  (closed) at  $Q^2 = 3 \text{ GeV}^2$ , CCFR [40], 1993.

In fact the analysis of Chyla and Kataev [42] led to  $\alpha_s^{NNLO}(M_Z) = 0.115 \pm .001 \pm .005 \pm .003 \pm .0005$  (errors: due to statistics, systematics, higher twist and scheme dependence). This value is well compatible and competitive with the world average from scaling violations in DIS:  $\alpha_s(M_Z) = 0.112 \pm .002 \pm .004$  [43].

It would be desirable to get  $\alpha_s(Q^2)$  by evaluating this sum rule at different momentum transfers (see also [33]).

## 6. $F_2$ at HERA

A new regime of deep inelastic scattering (DIS) was opened at HERA, where the range of  $Q^2$  and  $1/x$  is increased by about a factor 100 compared to previous experiments. At high  $Q^2$  ( $\gtrsim 1000 \text{ GeV}^2$ ),  $x$  is in the range of previous fixed target experiments and the new cross sections are predicted by perturbative QCD on the basis of the previous ones. This allows for stringent QCD tests.

In the new small  $x$  domain ( $x < 10^{-3}$ ), on the other hand, the techniques of QCD calculations are under study, as terms  $\log(1/x)$  may get important in the perturbative expansion. Furthermore new phenomena may appear due to very high parton densities.

Already in 1974 it was derived (double logarithmic asymptotic scaling [44]) that  $F_2$  rises versus small  $x$  at high  $Q^2$  faster than any power of  $\log(1/x)$ , but slower than any power of  $1/x$ . A strong rise of  $F_2$  at small  $x$  could also be expected due to the BFKL equations [45], which predict a growth of the gluon density like  $1/\sqrt{x}$  by leading  $\log(1/x)$  summation. On the other hand, the more traditional QCD fits based on linear  $Q^2$ -evolution equations (DGLAP [46]), which were so successful on former data, have little predictive power for the  $x$  dependence unless further assumptions are made.

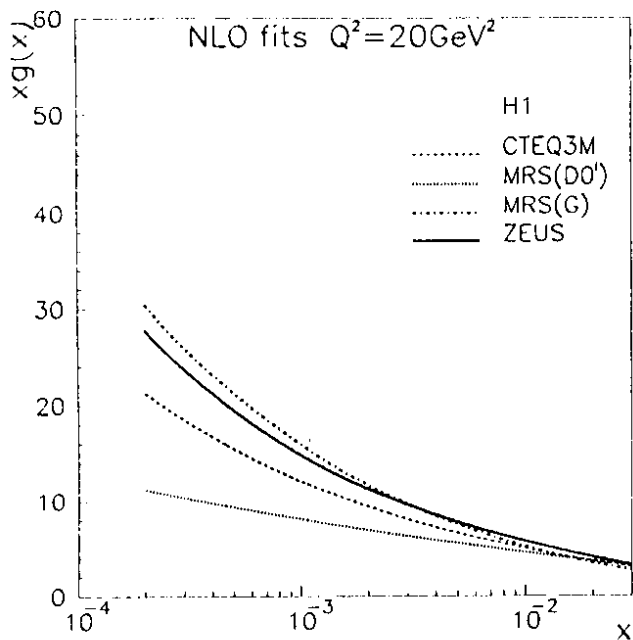


Figure 11. Gluon density  $xg(x)$  at  $Q^2 = 20 \text{ GeV}^2$  from next-to-leading order QCD fits. Results from H1 (error-band) and ZEUS [50] together with the parametrizations CTEQ3M, MRS(DO') and MRS(G). From [52]

The H1 and ZEUS collaborations reported indeed a strong rise of  $F_2$  at small  $x$  on the basis of data taken in 1992 [47], the first year of HERA operation. Now final

analyses of the 1993 data are available [48, 49], which confirm the former results. At small  $x$  a strong rise of  $xg(x)$ , where  $g(x)$  is the gluon density, like  $x^{-\delta}$ , with  $\delta$  in the range 0.2 to 0.4, is deduced from QCD analyses of these data [50, 51, 52]. (figure 11).

For strongly increasing gluon densities, saturation effects were expected and discussed since 1981 [53]. According a simple estimate [54] the proton is densely packed with gluons if the  $xg(x) \approx 6Q^2$  ( $Q^2$  in  $\text{GeV}^2$ ). Measured is only about 1/3 of that.

The data are remarkably well described by fits based on the DGLAP evolution equations and no experimental evidence for a BFKL mechanism can be claimed yet. For further details on the actual data, the quality of the QCD fits etc. see [55].

It might well be possible that the analysis of the hadronic final state sheds some light on these questions due to different ordering of parton energies and parton transverse momenta in the different QCD evolution schemes (see [56, 57]).

## 7. Quark and Gluon Jets and the Determination of $\alpha_s$

### 7.1. Early Jet Observations

Jets in the sense of a spray of hadrons as materialisation of quarks were first observed in 1975 [58] at the SPEAR  $e^+e^-$  accelerator. Gluon jets got "visible" in 1979 by clean 3 jet events (figure 12) [59] at PETRA.

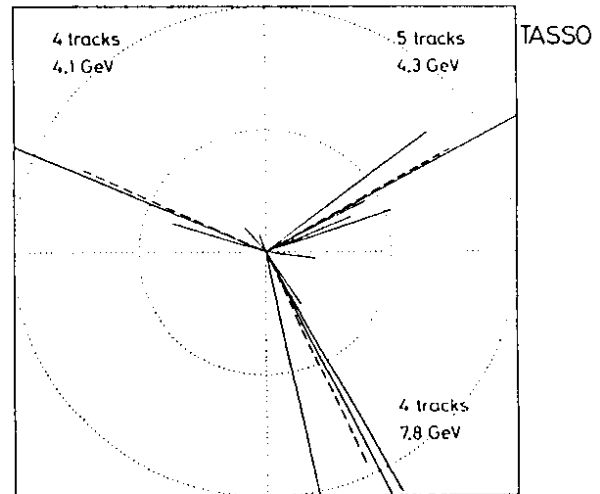


Figure 12. One of the first 3 jet event observed in  $e^+e^-$  at PETRA [59], 1979.

In DIS the situation was less clear due to the smaller available centre of mass energies and/or smaller angular acceptance for final state hadrons. Nevertheless, in the years around 1980 it was considered as a very important task to search for the patterns predicted by perturbative



QCD for the hadronic final state, with the hope to support the quantitative QCD tests performed in fully inclusive DIS (detecting only the final state lepton).

a) Increase of  $p_t$

From gluon emission a sizable increase with  $W$  of the transverse momenta of hadrons with respect to the axis given by the virtual photon and incident proton was expected [60] and also seen in  $\nu$  [61] and  $\mu$  [62] scattering. The results (figure 13) for different  $z = p \cdot p^{had} / p \cdot q$  were well described by models [63] which included QCD matrix elements to order  $\alpha_s$  (figure 14).

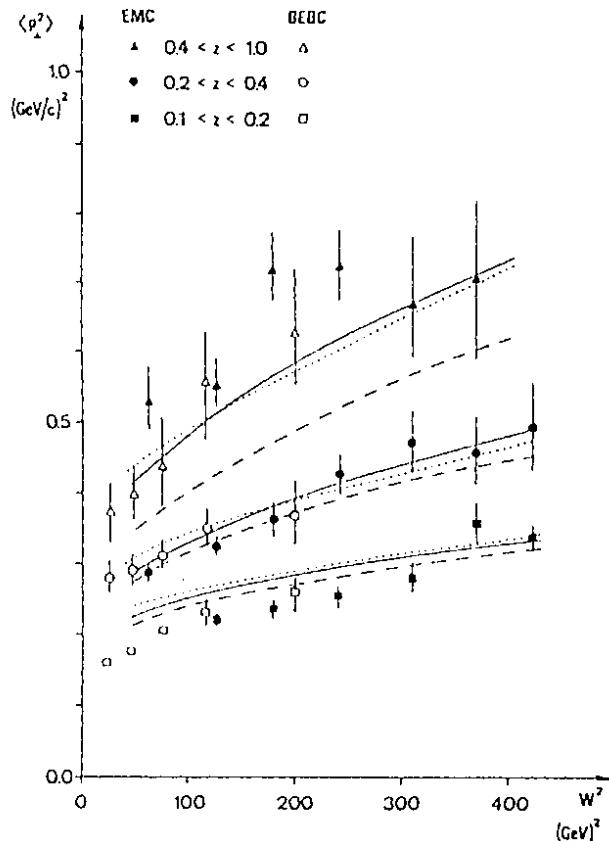


Figure 13.  $\langle p_t^2 \rangle$  of hadrons in  $\mu$  and  $\nu$  scattering for 3 ranges of  $z$  as function of  $W^2$ , 1980. Curves: Lepto-model including first order QCD matrix elements with different assumptions on transverse intrinsic quark momenta [63].

b) Event Shape

As already observed in  $e^+e^-$  interactions, flat events were expected in the hadronic centre of mass system (CMS) due to gluon emission. Such events and the favoured plane of hadrons were searched for by minimizing the summed  $p_t^2$  out of this plane [64]. Strong tails were observed in the distribution of the  $p_t^2$ -sum in the event plane (figure 15,b)) which again were well described by inclusion of QCD matrix elements of order  $\alpha_s$  in the Lepto Monte Carlo model [65], but could not easily be reproduced just by different assumptions on

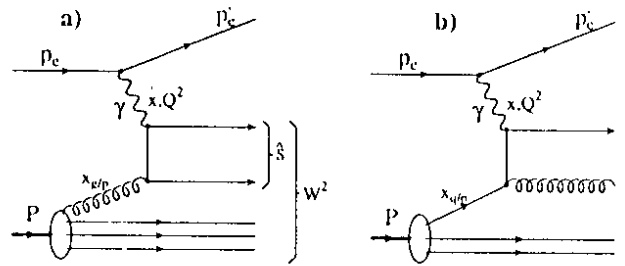


Figure 14. Diagrams for photon-gluon fusion (a) and the QCD Compton process (b) in first order of QCD.

the fragmentation process.

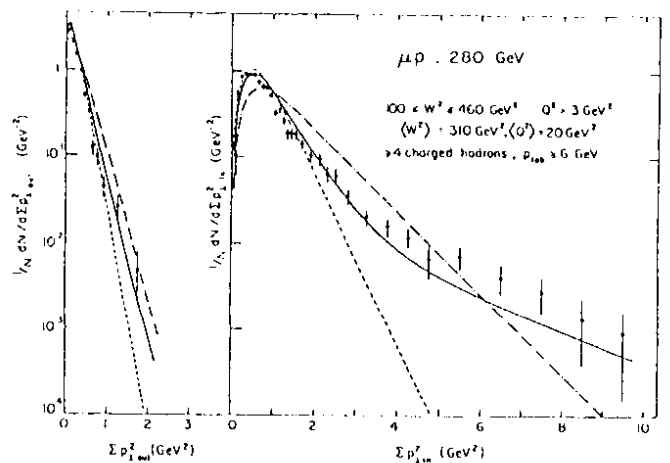


Figure 15. Distributions  $\sum p_t^2$  out of and in the favoured plane of hadrons. Solid line: Lepto model. [65] Dashed line and dashed dotted lines: Quark jet fragmentation assuming standard or large  $p_t$  due to fragmentation ( $\sigma_q = 310 MeV$  and  $\sigma_q = 470 MeV$ ). From EMC [64], 1981.

c) Energy Flow in the Event Plane

The flow of energy in the event plane (section b) above) in the forward hemisphere of the hadronic CMS was shown [64] to be collimated versus the forward (virtual  $\gamma$  direction), corresponding to a current jet structure (figure 16,a)). If however events are selected which contain a high  $p_t$  particle (figure 16,b)), a structure evolves which can be interpreted as the pattern of two forward jets (the proton remnant jet is not accepted). Indeed such a structure was predicted in the Lepto model, if first order QCD matrix elements were included.

To summarize, the details of the hadronic final state (points a) to c)) as observed in the early eighties gave very satisfying qualitative support to the quantitative QCD analyses performed in inclusive lepton scattering.

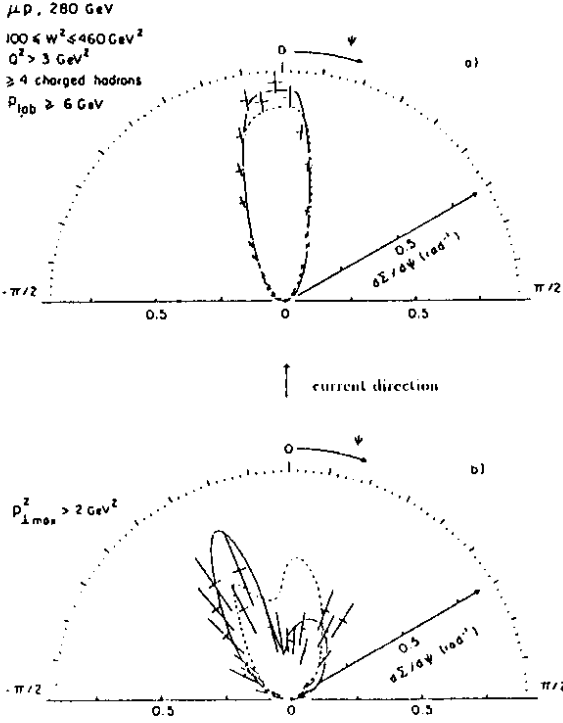


Figure 16. Flow of scaled charged hadron energy  $\langle z \rangle / \text{rad}$ , where  $z = p \cdot p^{\text{had}} / p \cdot q$ . In b)  $\geq 1$  track is required with  $p_t^2 > 2 \text{ GeV}^2$ . Solid line: Lepto model. [65] Dashed line: Quark jet fragmentation assuming small large  $p_t$  due to fragmentation ( $\sigma_q = 470 \text{ McV}$ ). From EMC [64], 1981.

### 7.2. First Jet analyses in DIS

The E665 collaboration at Fermilab was, to my knowledge, the first to apply jet algorithms to data in DIS [66]. Events with “(2+1)” jets (2 observed jets +1 proton remnant jet) were reconstructed using the JADE algorithm [68]. The observed jet rates and other observables were shown to be in agreement with QCD based models, comparable to the results of section 7.1.

A big next step was a determination of  $\alpha_s(Q^2)$  [67]. The  $E_t$  distribution of jets was evaluated on the basis of a leading order QCD calculation [60]. The resulting  $\alpha_s(Q^2)$  is shown in figure 17 in comparison to other determinations. The E665 results fit beautifully into the general picture, but the questions remain, whether the process is hard enough for a reliable perturbative QCD calculation ( $\langle E_t \rangle \approx 3 \text{ GeV}^2$  for the 2 observed jets), whether the reconstructed jets can directly be identified with partons, and what the influence of next to leading order corrections might be.

### 7.3. Jet analyses and $\alpha_s$ determination at HERA

Due to the increase of  $W^2$  by about a factor 100 compared to fixed target experiments, the jets at

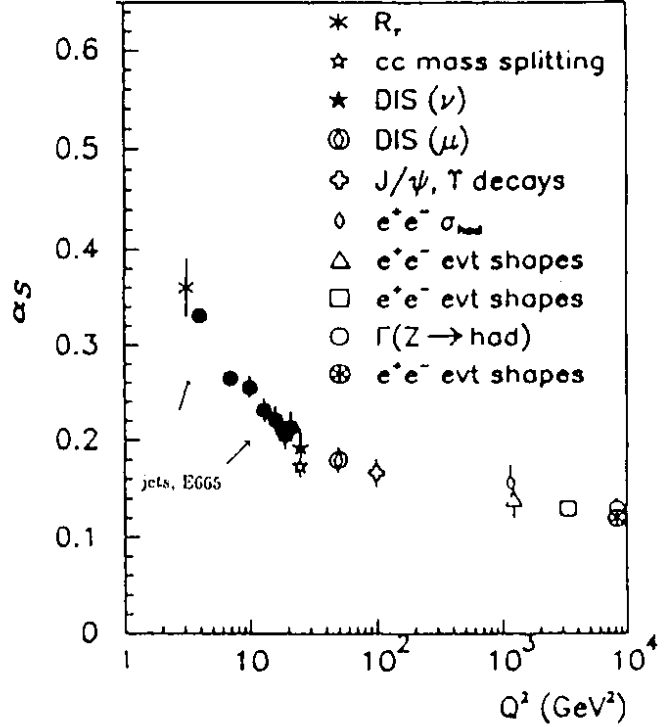


Figure 17.  $\alpha_s$  vs.  $Q^2$  or vs.  $s$  in case of  $e^+e^-$ . Results of E665: solid points [67].

HERA have enough phase space to show up as distinct structures. Jet-jet masses are typically 20 GeV using e.g. the JADE algorithm [68] with a jet resolution parameter  $y_{\text{cut}} \approx 0.02$  with  $m_{\text{jet, jet}}^2 > y_{\text{cut}} W^2$ . Clean jet structures are seen in the energy flow with respect to the reconstructed jet axis (figure 18, [69]) or also in individual events (figure 19).

The crucial point in the determination of  $\alpha_s$  from the observed multi jet rates is the reliable reconstruction of the underlying parton kinematics from the observed hadrons event by event. The Monte Carlo Model mostly used so far for this purpose is the LEPTO generator [70], which contains in the “MEPS” option the QCD matrix elements (ME) to order  $\alpha_s$  (figure 14) and “leading log” parton showers (PS) to describe approximately higher order effects.

The remaining problems are

- the model dependence in the corrections from jets to partons,
- the approximations in the treatment of the parton showers and their matching to the calculation based on the matrix elements.

Nevertheless the H1 collaboration determined  $\alpha_s(Q^2)$  [71] on the basis of a next to leading order calculation of the (2+1)-jet rate (2 observed jets +1 proton remnant jet) using the program PROJET of D. Graudenz [72].

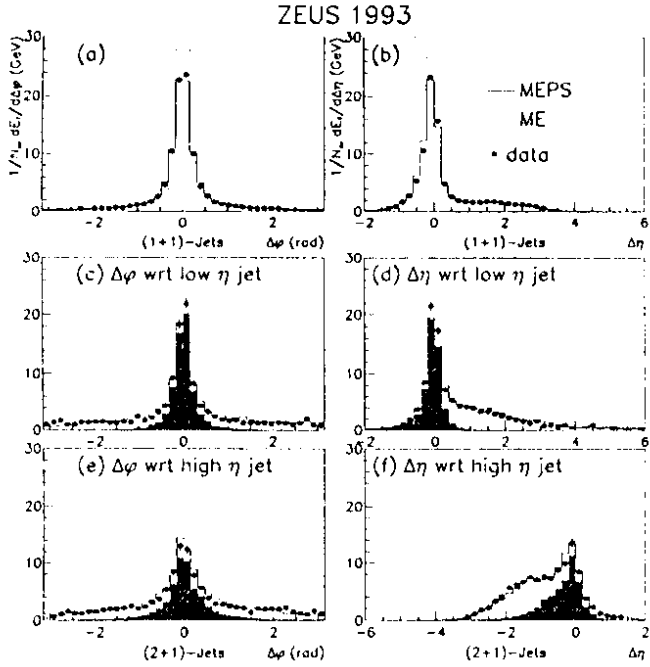


Figure 18. Transverse energy flows in the HERA frame relative to the reconstructed jet directions for (1+1)-jet (a,b) and (2+1)-jet events (c-f).  $160 < Q^2 < 1280 \text{ GeV}^2$ ,  $0.01 < x < 0.1$ . The solid histograms shows the energies attributed to the jets by the jet algorithm. From [69].

To remove the uncertain influence of parton showers in the Monte Carlo corrections and to depend less on the fragmentation of the proton remnant, a cut  $\theta_{jet} > 10^\circ$  was introduced, where  $\theta_{jet}$  is the polar angle of the jets with respect to the proton beam in the lab frame.

In figure 20,  $\alpha_s(Q^2)$  is shown as function of  $Q^2$  as deduced from the fraction of 2+1-jet events. Indeed  $\alpha_s$  is "running" as expected on the basis of QCD. A value  $\alpha_s(M_Z) = 0.123 \pm 0.018$  was determined from the points at  $Q^2 > 100 \text{ GeV}^2$ . Here the model dependence of the corrections is reduced. The result compares well with results from LEP,  $\alpha_s(M_Z) = 0.119 \pm 0.010$ , obtained from similar observables [73]. The HERA result adds nothing in precision to LEP, but the comparison is a relevant QCD test, as the two results are obtained from different QCD processes with either large time like or space like virtual photon masses which set the renormalization scale.

The ZEUS collaboration has presented a very detailed paper [69] on jet measurements at high  $Q^2$ . In particular for (2+1)-jet events the scaling variables  $x_p$  and  $z$  were studied with

$$x_p = Q^2/2\xi p \cdot q = x_{Bj}/\xi = \frac{Q^2}{Q^2 + \hat{s}},$$

where  $\xi$  is the momentum fraction of the incident

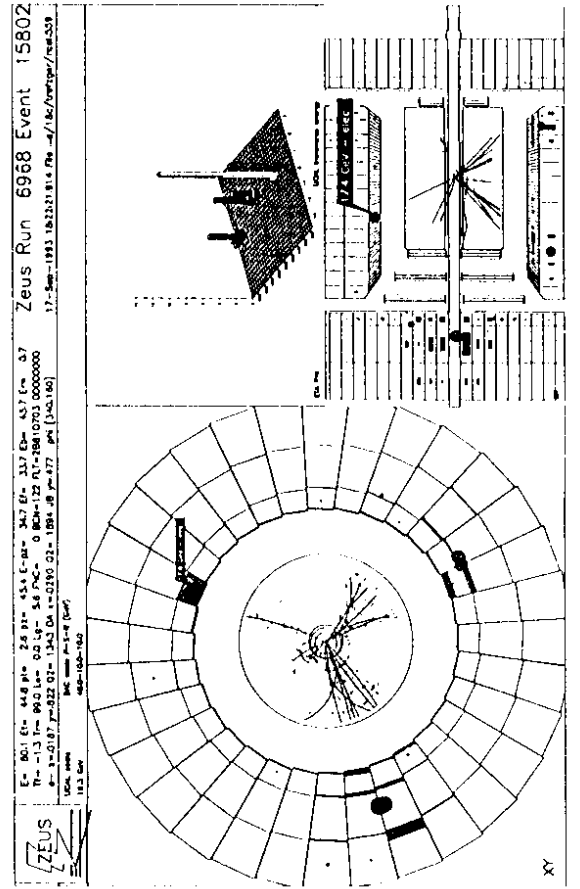


Figure 19. (2+1) jet event in the ZEUS detector. Upper graph: side view of the detector, the p beam coming from top (in the figure). The lego plot shows the energy flow (electron in white, jets in black). Lower graph: view along the beam.

proton, which enters the hard scattering process, and

$$z = p \cdot p_{jet} / p \cdot q \approx \frac{E_{jet}(1 - \cos(\theta_{jet}))}{\sum_{i=1}^2 E_{jet}^i(1 - \cos(\theta_{jet}^i))}$$

It is shown in figure 21 that the Monte Carlo models and also the NLO PROJET calculation describe the data quite well besides the region of  $z < 0.1$ , where one of the 2 jets is close to the proton beam direction. The H1 collaboration has removed this uncertain region by the cut  $\theta_{jet} > 10^\circ$  (see above). ZEUS at this stage [69] refrained to determine  $\alpha_s$  in view of this discrepancy with PROJET.

This is certainly not the end of the story and already at this workshop new analyses have been presented [74, 56].

## 8. Electroweak Effects in $eN$ scattering

Electron nucleon scattering is dominated by the electromagnetic one photon exchange at  $Q^2 \lesssim M_Z^2$ . To observe

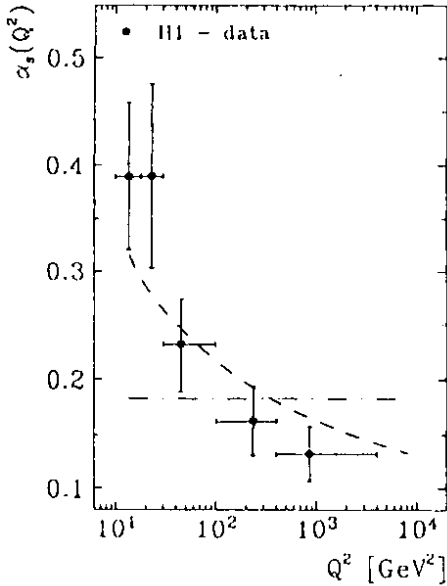


Figure 20.  $\alpha_s(Q^2)$  and fit according the renormalization group equation and for comparison also to a constant  $\alpha_s$  (from [71]).

weak effects, either extreme precision is needed or very high energies must be available as e.g. at HERA.

### 8.1. Parity non-conservation in $ed$ scattering

One of the high lights of electron scattering was the observation of parity violation in  $ed$  scattering in 1978 at SLAC [75]. Longitudinally polarized electrons were scattered from an unpolarized deuterium target (figure 22). Only a tiny polarization asymmetry of  $A \approx 10^{-4}Q^2$ , with  $1 < Q^2 < 1.9 \text{ GeV}^2$ , was expected. Therefore extreme statistical accuracy and very small systematical errors were required.

A Gallium-Arsenide source, pumped by circularly polarized laser light, supplied electrons with a polarization of 37%. The sign of the polarization could be changed randomly on a pulse to pulse basis. After acceleration about  $10^5$  electrons were scattered per sec into a magnetic spectrometer (figure 22). They were not counted, but the output currents of a Čerenkov and a "shower counter" (calorimeter) were integrated. It could be demonstrated on the  $10^{-5}$  level that the asymmetry followed the changing orientation of the electron spin, both by polarization changes at the source and due to the  $g - 2$  electron spin precession in the  $24.5^\circ$  deflection in the beam, which led to different spin orientations at the target as function of beam energy.

The measured asymmetry

$$A/Q^2 = (-9.5 \pm 1.6) 10^{-5} \text{ GeV}^{-2}$$

showed that electrons indeed prefer to scatter left handed as predicted by the Glashow-Salam-Weinberg (GSW) electroweak theory. The Weinberg angle was deduced corresponding to

$$\sin^2\theta_W = 0.20 \pm 0.03$$

This beautiful experiment gave important support for the electroweak theory, well before the confirmations at the  $pp$  and  $e^+e^-$  colliders.

At HERA large effects in such asymmetry measurements at  $Q^2 \approx 10^4 \text{ GeV}^2$  are expected and will be measurable with polarized electrons and luminosities of order  $10\text{pb}^{-1}$ .

### 8.2. Search for effects of the propagator mass in charged current interactions

Already in the sixties people searched for deviations of the total  $\nu N$  cross section from the linear rise proportional to energy as a trace of an exchanged particle ("IVB", intermediate vector boson, at the time) in charged-current (CC) interactions. That the mass of the exchanged particle was far too heavy to be observed that way, could be understood only after the

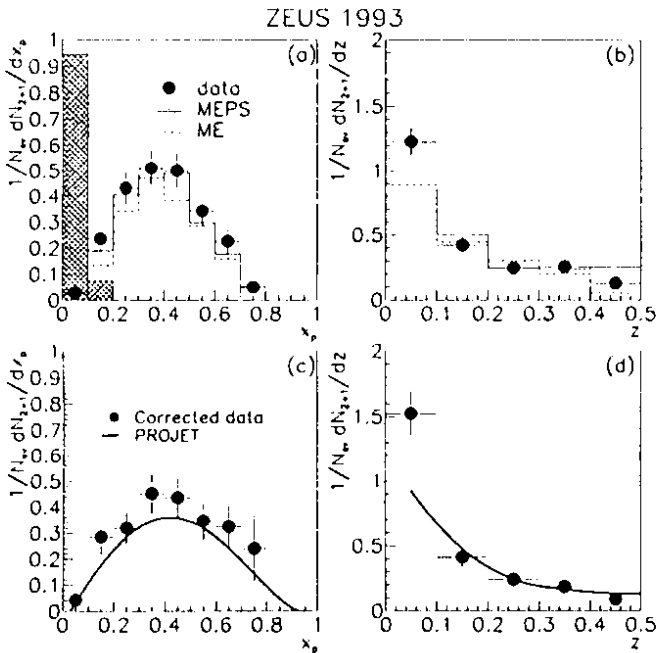


Figure 21. Distribution of uncorrected (2+1) jet events vs  $x_p$  and  $z$  compared to the LEPTO Monte Carlo in the MEPS and ME options (a), and the same corrected to the parton level compared to PROJET (b) for  $160 < Q^2 < 1280 \text{ GeV}^2$ ,  $0.01 < x < 0.1$ . The shaded histogram in a) shows the corresponding distribution for  $10 < Q^2 < 20 \text{ GeV}^2$ ,  $0.0012 < x < 0.0024$  for comparison. From [69].

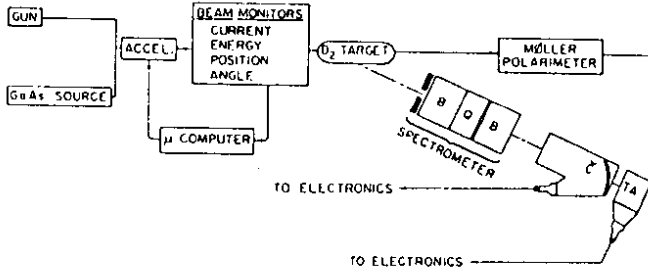


Figure 22. Experimental set-up at SLAC, 1978, for  $ed$  scattering with polarized beam and unpolarized target [75].

the discovery in 1973 [76] of weak neutral current (NC) interactions.

At the 1976 Rencontres Moriond, V. Brisson presented [77] an analysis of NC  $\nu N$  and  $\bar{\nu} N$  from the Gargamelle bubble chamber [78].

Assuming V and A couplings the NC cross section can be written

$$\frac{d\sigma(\nu N)}{dy} = \frac{G_F M_N E_\nu}{\pi} (A_L + A_R(1-y))^2$$

$$\frac{d\sigma(\bar{\nu} N)}{dy} = \frac{G_F M_N E_{\bar{\nu}}}{\pi} (A_L(1-y)^2 + A_R)$$

The Gargamelle result (figure 23) for the left and right handed couplings  $A_L$  and  $A_R$  excluded pure  $\Lambda, V, V+A$  and also  $V-A$  theories, and this gave strong support to the GSW model. That the mass of the exchanged boson was very heavy was than obvious from the resulting Weinberg angle ( $\sin^2\theta_W = 0.28 \pm 0.05$ ) from which the  $W$  mass could be calculated as

$$M_W^2 = (37.3 \text{ GeV})^2 / \sin^2\theta_W \approx (70 \text{ GeV})^2$$

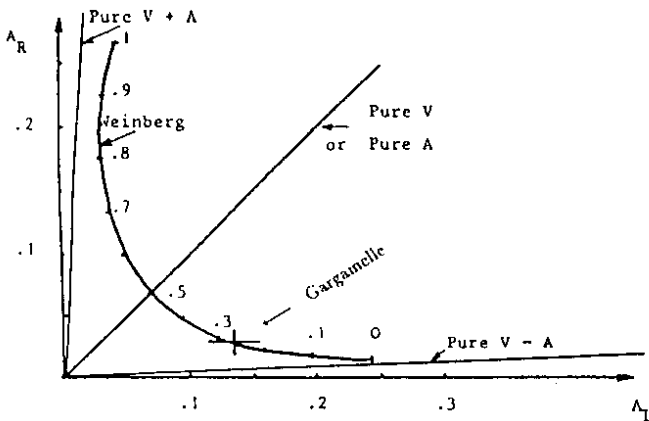


Figure 23. Determination of Right handed and left handed couplings from neutral current  $\nu$  data of the Gargamelle bubble chamber as presented in [77], 1976.

At HERA CC interactions are studied by the inverse

neutrino interactions

$$e^- p \rightarrow \nu_e X \quad \text{and} \quad e^+ p \rightarrow \bar{\nu}_e X$$

The impressive event at  $Q^2 \approx 20000 \text{ GeV}^2$  shown in figure 24 illustrates that such CC events can be detected by hadron jets with large missing transverse momentum due to the escaping  $\nu$  or  $\bar{\nu}_e$ .

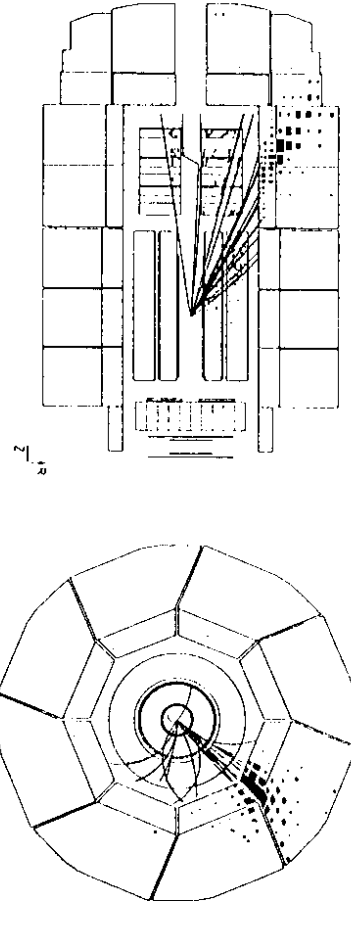


Figure 24. event of the reaction  $e^+ p \rightarrow \nu_e X$  in the H1 detector. Top: sideview,  $p$  beam from below (in figure). Bottom: View along  $p$  beam.

The reduction of the total cross section by the  $W$ -propagator can be seen at HERA energies (figure 25) [79]. It could also be demonstrated [80] (figure 26) that at momentum transfers  $Q^2$  of order  $M_W^2, M_Z^2$  the  $ep$  NC and CC cross sections are of similar magnitude, quite different from low  $Q^2$ , where, due to photon exchange, NC dominates over CC by about a factor 1000.

Furthermore it was measured [81] that the cross section for  $e^- p \rightarrow \nu_e X$  is about 2.3 times larger than that for  $e^+ p \rightarrow \bar{\nu}_e X$  for the given kinematics at HERA, in agreement with the expectation from the standard

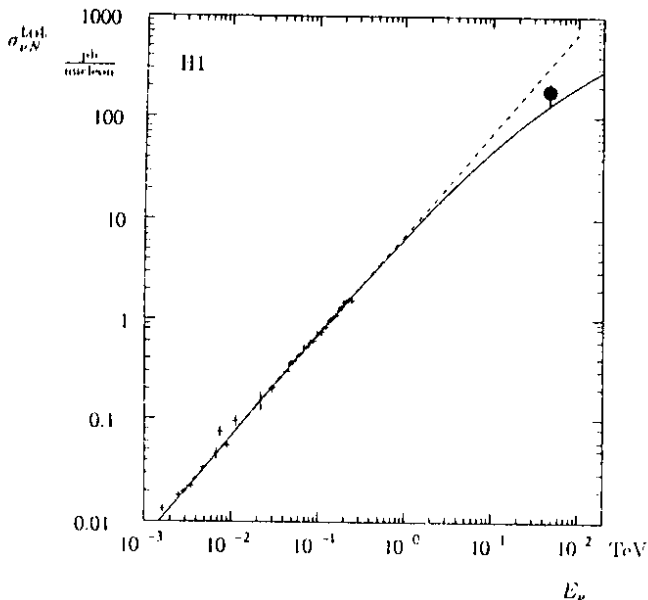


Figure 25. Energy dependence of  $\nu N$  cross section. The solid point is the conversion of the result on  $e^-p \rightarrow \nu_e X$  at HERA ([79]).

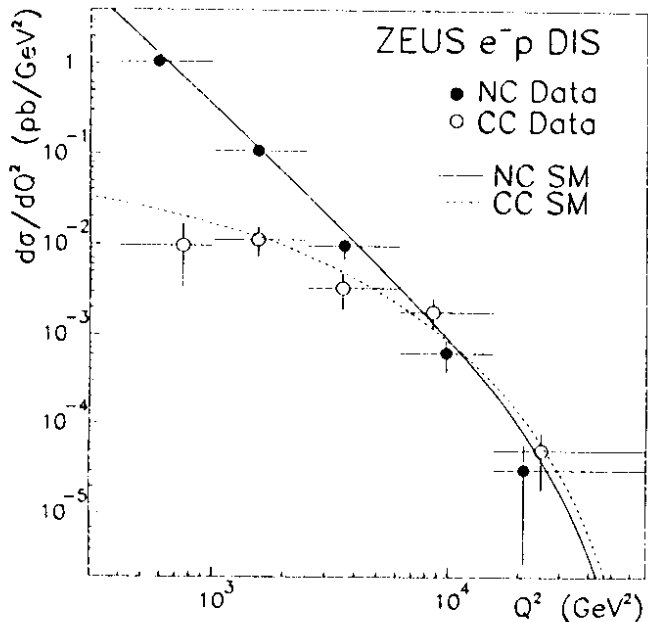


Figure 26. Neutral current (solid) and charged current (open)  $e^-p$  cross section as function of  $Q^2$  [80].

model taking into account the quark content of the proton and the couplings of  $W^+$  and  $W^-$ .

The measurements at HERA of electroweak phenomena are just starting and have not reached the precision of  $e^+e^-$  and  $p\bar{p}$  collider and fixed target  $\nu$  experiments. The results are however very valuable already now, as the standard model is tested at large space like momentum transfers, a regime little explored so far.

## 9. Concluding Remarks

Looking back into the history of deep inelastic scattering, we notice that the most important discoveries were made in the late sixties and early seventies. Starting with scaling (1968-69), assignment of spin 1/2 to the constituents (1969), discovery of weak neutral currents (1973) up to scaling violations (1974), the most fundamental observations of DIS were made in a few years. Looking aside, we notice that in this productive time also the  $c$ -quark was finally discovered in 1974 (having left some traces long before in di- $\mu$ -events in  $\nu$  scattering, in the Drell-Yan process and in  $R$  in  $e^+e^-$ ) and the  $\tau$  lepton in 1975. The eighties saw less unexpected experimental effects in DIS, to mention are in particular the nuclear "EMC-effect" (1983) and the EMC results on the nucleon spin of 1988.

In the late seventies and eighties the patterns predicted by QCD were beautifully borne out by the experiments which produced precision data on  $F_2$  and  $F_3$  in a wide kinematical range. But the basic theoretical concepts of QCD had been developed already in 1972-1973. Even the DGLAP and BFKL evolution equations, the applicability of which to low  $x$  data we just discuss, are around 20 years old by now. Saturation due to high gluon densities was discussed already in 1981 [53]. Similarly, to probe the pomeron structure as done recently at HERA [82] was proposed already 10 years before [83].

However the basic old theoretical concepts do not allow for firm predictions in all the new HERA regime. For example the rise of  $F_2$  and the gluon density at low  $x$  came for many as a surprise, in spite of general QCD based arguments [44]. Similarly the phenomena of final states, e.g. jet ordering or patterns of diffraction are difficult to predict from basic QCD principles, but experimental data may clarify the appropriate application of them.

At high  $Q^2$ , HERA provides stringent tests of QCD and of the electroweak theory, both in structure functions and by the analysis of the hadronic final state, with increasing precision in the forthcoming years.

HERA has a very rich and interesting program from which I mentioned only a fraction in this talk. I therefore think we are in the proper time and town to update the the very old judgement of Paris: "Hera is most beautiful".

## Acknowledgements

It is a great pleasure to thank the organizers for a stimulating workshop. I am grateful to J. Meyer for reading the manuscript and useful suggestions.

## References

- [1] R. Hofstadter, *Electron Scattering and Nuclear and Nucleon Structure*, Benjamin, New York, 1963.
- [2] W. Albrecht et al., Phys. Rev. Lett. 17 (1966) 1192.
- [3] A.A. Cone et al., Phys. Rev. 156 (1967) 1490.
- [4] J.D. Bjorken, Phys. Rev. 148 (1966) 1467.
- [5] F.W. Brasse et al., DESY report 67/34 (1967), W. Albrecht et al., ibid. 68/48 (1968), and with less detail in Nuovo Cimento A55 (1968) 679, Phys. Lett. 28B (1968) 225.
- [6] W. Panofsky, Proc., 14th Conf. on HEP, Vienna, 1968, p.23
- [7] J.D. Bjorken, Phys. Rev. 179 (1969) 1547.
- [8] E.D. Bloom et al., Phys. Rev. Lett. 23 (1969) 930.
- [9] W. Albrecht et al., Nucl. Phys. Rev. B13 (1969) 1.
- [10] C.G. Callan and D.J. Gross, Phys. Rev. Lett. 22 (1969) 156
- [11] W. Albrecht et al., contributed paper to the 4<sup>th</sup> Int. Symp. on Electron and Photon Interactions, Liverpool, 1969 and DESY report 69/46 (1969) (unpublished); R.E. Taylor, Proceedings same conference, p. 251.
- [12] E.D. Bloom, F.J. Gilman, Phys. Rev. Lett. 25 (1970) 1140.
- [13] D.J. Fox et al., Phys. Rev. Lett. 33 (1974) 1504., Y. Watanabe et al., Phys. Rev. Lett. 35 (1975) 898.
- [14] E.M. Riordan et al., SLAC PUB 1634, August 1975 (unpublished).
- [15] H.L. Anderson et al., Phys. Rev. Lett. 38 (1977) 1459; B.A. Gordon et al., Phys. Rev. Lett. 41 (1978) 615.
- [16] J.D. Bjorken, E.A. Paschos, Phys. Rev. 185 (1969) 1975
- [17] C. Llewellyn Smith, Nucl. Phys. B17 (1970) 277.
- [18] J. Kuti and V. Weisskopf, Phys. Rev. D4 (1971) 3418.
- [19] D. H. Perkins, Proc., 1975 Int. Symp. of Lepton and Photon Interactions, p. 571.
- [20] H.L. Anderson et al., Phys. Rev. Lett. 40 (1978) 1061.
- [21] BEBC Coll., P.C. Bossetti et al., Nucl. Phys. B142 (1978) 1 CDHS Coll., J.G.H. de Groot et al., Z. Phys. C1 (1979) 143.
- [22] M. Glück and E. Reya, Nucl. Phys. B156 (1979) 456.
- [23] EMC, J.J. Aubert et al., Phys. Lett. B123 (1983) 275.
- [24] A. Bodek et al., Phys. Rev. Lett. 50 (1983) 1431.
- [25] A. Bodek et al., Phys. Rev. Lett. 51 (1983) 534.
- [26] NMC, P. Amaudruz et al., Z. Phys. C51 (1991) 387.
- [27] M. Ericson, A.W. Thomas, Phys. Lett. B128 (1983) 112; C.H. Llewellyn Smith, ibid., p. 107.
- [28] M. Arneodo, Phys. Rept. 240 (1994) 301.
- [29] Plenary talks of A. Bialas and P. Hoyer and talks in working group 4, these proceedings.
- [30] M. Virchaux, Proc., "QCD, 20 years later", Aachen, 1992, p. 205.
- [31] R. Voss, Proc., 16<sup>th</sup> Int. Symp. on Lepton and Photon interactions, Ithaca, 1993, p. 144.
- [32] J. Feltesse, DAPNIA-SPP-94-35 (1994), Proc., 27<sup>th</sup> Int. Conf. on HEP, Glasgow, 1994.
- [33] H. Schellman, this proceedings.
- [34] K. Gottfried, Phys. Rev. Lett. 18 (1967) 1174; R.D. Field and R.P. Feynman, Phys. Rev. D15 (1977) 2590.
- [35] NMC, P. Amaudruz et al., Phys. Rev. Lett. 66 (1991) 2712; NMC, M. Arneodo et al., Phys. Rev. D50 (1994) 1.
- [36] NA51 Collab., A. Baldit et al., Phys. Lett. B332 (1994) 244.
- [37] CDF Collab., F. Abe et al., Phys. Rev. Lett. 74 (1995) 850.
- [38] F. Willeke, these proceedings.
- [39] D.J. Gross and C.H. Llewellyn Smith, Nucl. Phys. B14 (1969) 337.
- [40] CCFR Collab., W.C. Leung et al., Phys. Lett. B317 (1993) 655.
- [41] S.A. Larin and J.A.M. Vermaseren, Phys. Lett. B259 (1991) 345.
- [42] J. Chyla and A.L. Kataev, Phys. Lett. B297 (1992) 385.
- [43] Particle Data Group, Phys. Rev. D50 (1994) 1173.
- [44] A. De Rujula et al., Phys. Rev. D10 (1974) 1649.
- [45] E.A. Kuraev, L.N. Lipatov, V.S. Fadin, Sov. Phys. JETP 45 (1972) 199; Y.Y. Balitsky, L.N. Lipatov, Sov. J. Nucl. Phys. 28 (1978) 282.
- [46] V.N. Gribov and L.N. Lipatov, Sov. Journ. Nucl. Phys. 15 (1972) 438 and 675; G. Altarelli and G. Parisi, Nucl. Phys. B126 (1977) 298; Y.L. Dokshitzer, Sov. Phys. JETP 46 (1977) 641.
- [47] H1 Collab., I. Abt et al., Nucl. Phys. B407 (1993) 515; ZEUS Collab., M. Derrick et al., Phys. Lett. B316 (1993) 412.
- [48] ZEUS Collab., M. Derrick et al., Z. Phys. C65 (1995) 379.
- [49] H1 Collab., T. Ahmed et al., Nucl. Phys. B439 (1995) 471.
- [50] ZEUS Collab., M. Derrick et al., Phys. Lett. B345 (1995) 576.
- [51] A.D. Martin, W.J. Stirling, R.G. Roberts, RAL-95-021, (1995).
- [52] H1 Collab., S. Aid et al., DESY report 95-081 (1995), Phys. Lett. in print.
- [53] L.V. Gribov, E.M. Levin and M.G. Ryskin, Nucl. Phys. B188 (1981) 555 and Phys. Rep. 100 (1983).
- [54] A.H. Mueller, Nucl. Phys. B(Proc. suppl.) 18C (1990) 125.
- [55] Plenary talk, P. Kooijman and talks in working group 1, these proceedings.
- [56] M. Kuhlén, these proceedings.
- [57] H1 Collab., S. Aid, et al., DESY preprint 95-108 (1995), Phys. Lett. in print; A. De Roeck; T. Haas, these proceedings.
- [58] G. Hanson, Phys. Rev. Lett. (1975) 1609.
- [59] Tasso Collab., Proc. 9<sup>th</sup> Int. Symp. on Lepton Photon Interactions, Batavia, 1979, p. 34.
- [60] G. Altarelli and G. Martinelli, Phys. Lett. 76B (1978) 89.
- [61] ABCDLOS Collab., H. Deden et al., Nucl. Phys. B181 (1981) 375.
- [62] EMC, J.J. Aubert et al., Phys. Lett. 95B (1980) 306.
- [63] Bo Andersson et al., Z. Phys. C9 (1981) 233.
- [64] EMC, J.J. Aubert et al., Phys. Lett. 100B (1981) 433.
- [65] G. Ingelman and T. Sjöstrand, LU TP 80-12 (1980).
- [66] E665 Collab., M. R. Adams et al., Phys. Rev. Lett. 69 (1992) 1026.
- [67] E665 Collab., M.R. Adams et al., Phys. Rev. Lett. 72 (1994) 466.
- [68] JADE Collab., W. Bartel et al., Z. Phys. C33 (1986) 23.
- [69] ZEUS Collab., M. Derrick et al., DESY 95-16 (1995), Z. Phys. in print.
- [70] G. Ingelman, Proc. Workshop 'Physics at HERA', Hamburg, 1991, vol. 3, p. 1366
- [71] H1 Collab., T. Ahmed et al., Phys. Lett. B346 (1995) 415.
- [72] D. Graudenz, CERN-TH.7420/94, Phys. Rev. D49 (1994) 3291.
- [73] S. Bethke and J.E. Pilcher, Ann. Rev. Nucl. Science 42 (1992) 251.
- [74] B. Foster, these proceedings; G. Grindhammer, ibid.
- [75] C.Y. Prescott et al., Phys. Lett. 77B (1978) 347.
- [76] F.J. Hasert et al., Phys. Lett. 46B (1973) 138.
- [77] V. Brisson, Proc. of the Rencontres de Moriond, France 1976, vol. 2, p. 253.
- [78] see also discussion by D. Haidt, Nucl. Phys. B (Proc. Suppl.) 36 (1994) 387.
- [79] H1 Collab., T. Ahmed et al., Phys. Lett. B324 (1994) 241.
- [80] ZEUS Collab., M. Derrick et al., DESY 95-053 (1995), Phys. Rev. Lett. in print.
- [81] H1 Collab., S. Aid et al., DESY 95-102 (1995), Z. Phys. in print.
- [82] H1 collab., T. Ahmed et al., Phys. Lett. B348 (1995) 681; ZEUS collab., M. Derrick et al., DESY 95-93 (1995), submitted to Z. Phys.
- [83] G. Ingelman and P. Schlein, Phys. Lett. B152 (1985) 256.